

Supporting information
for

Bis-cycloheptyl-fused bis(imino)pyridine-cobalt catalysts for PE wax formation: positive effects of fluoride substitution on catalytic performance and thermal stability

Qiuyue Zhang,^{†,‡} Ningning Wu,[†] Junfeng Xiang,[†] Gregory A. Solan,^{*,†,§} Hongyi Suo,^{†,‡} Yanping Ma,^{*,†} Tongling Liang[†] and Wen-Hua Sun^{*,†,‡,#}

[†] Key Laboratory of Engineering Plastics and Beijing National Laboratory for Molecular Sciences, Institute of Chemistry, Chinese Academy of Sciences, Beijing 100190, China. E-mail: whsun@iccas.ac.cn; Fax: +86-10-62618239; Tel: +86-10-62557955.

[‡] CAS Research/Education Center for Excellence in Molecular Sciences and International School, University of Chinese Academy of Sciences, Beijing 100049, China.

[§] Department of Chemistry, University of Leicester, University Road, Leicester LE1 7RH, UK. E-mail: gas8@leicester.ac.uk. Tel: +44-116-2522096.

[#] State Key Laboratory for Oxo Synthesis and Selective Oxidation, Lanzhou Institute of Chemical Physics, Chinese Academy of Sciences, Lanzhou 730000, China.

Table of Contents

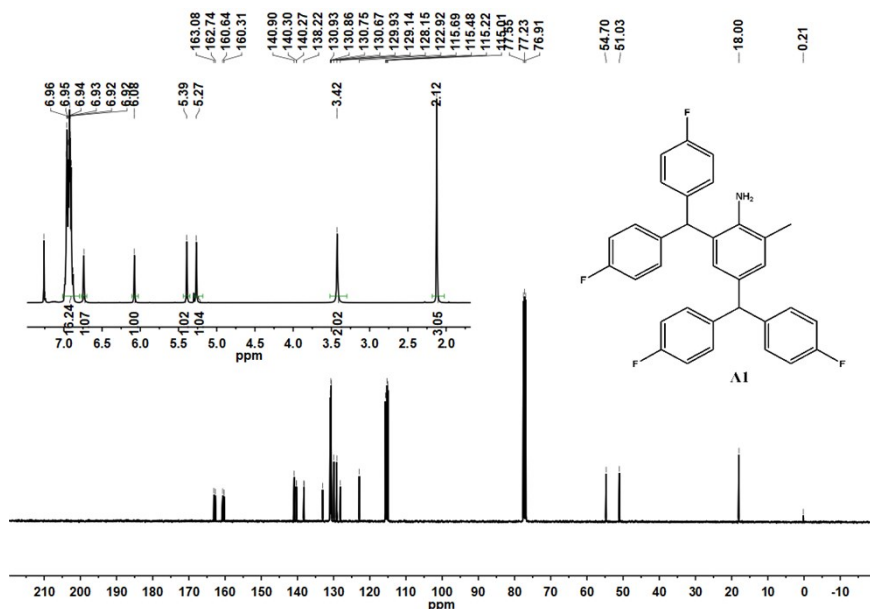
1. NMR data for the anilines, A1 – A7	S2
2. Figure S1 ¹⁹ F NMR spectra of Co1 , Co2 , Co3 , Co4 , Co6 and Co7 ; recorded in CDCl ₃ at ambient temperature.	S6
3. Figure S2 (a) GPC traces for the polymers obtained using Co5 /MMAO at various temperatures; (b) Plot of activity and M _w versus temperature for the catalyst and polyethylene, respectively (entries 1 – 6, Table 4).	S6
4. Figure S3 (a) GPC traces for the polymers obtained using Co5 /MMAO at various Al:Co molar ratios; (b) Plot of activity and M _w versus Al:Co molar ratio for the catalyst and polyethylene, respectively (entries 4, 7 – 10, Table 4).	S7
5. Figure S4 (a) GPC traces for the polymers obtained using Co5 /MMAO at various run times; (b) Plot of activity and M _w versus time for the catalyst and polyethylene, respectively (entries 4, 11 – 14, Table 4).	S7
6. Figure S5 Comparison of the catalytic activities and molecular weight of the polyethylenes generated using Co1 – Co7 and Co_{mes} ; MMAO used as co-catalyst in each case.	S7
7. Figure S6 ¹ H NMR spectrum of the polyethylene obtained using Co4 /MAO at 60 °C; recorded at 100 °C in 1,1,2,2-tetrachloroethane-d ₂ (entry 5, Table 3).	S8
8. Figure S7 ¹ H NMR spectrum of the polyethylene obtained using Co5' /MAO at 60 °C; recorded at 100 °C in 1,1,2,2-tetrachloroethane-d ₂ (entry 7, Table 3).	S8
9. Table S1 Crystal data and structure refinements for Co4 , Co5 , Co5' and Co5'' .	S9
10. References	S10

NMR data for the anilines, A1 – A7

Compounds A1 – A7 were synthesized based on related literature procedures.¹

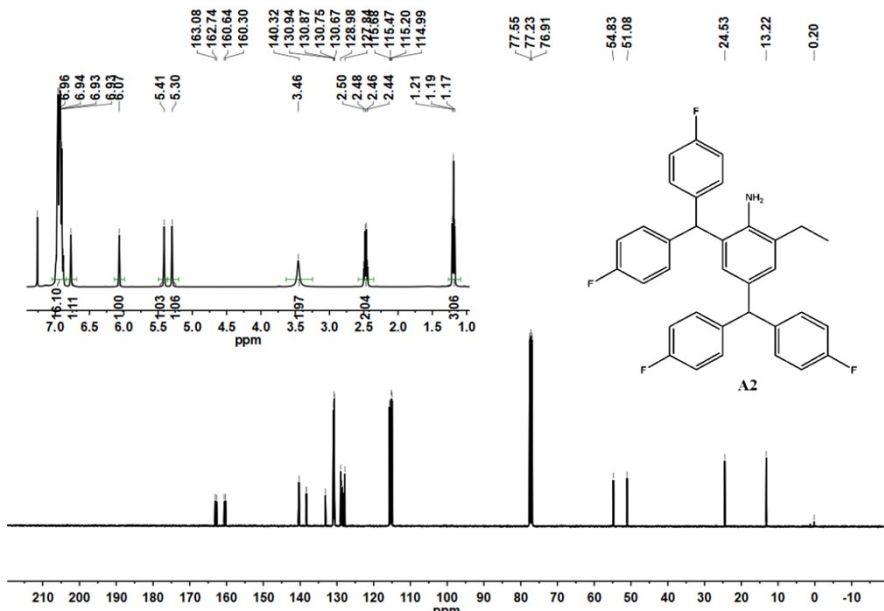
(a) ¹H and ¹³C NMR spectroscopic data for A1 – A7

2-Methyl-4,6-bis{di(*p*-fluorophenyl)methyl}aniline (A1, Yield: 59%)



Compound A1. ¹H NMR (400 MHz, CDCl₃, TMS): δ 6.98–6.88 (m, 16H), 6.74 (s, 1H, aryl-H), 6.08 (s, 1H, aryl-H), 5.39 (s, 1H, CH(*p*-FPh)₂), 5.27 (s, 1H, CH(*p*-FPh)₂), 3.42 (s, 2H, NH₂), 2.12 (s, 3H, CH₃). ¹³C NMR (100 MHz, CDCl₃, TMS): δ 163.08, 162.74, 160.64, 160.31, 140.90, 140.30, 140.27, 138.22, 138.19, 133.05, 130.93, 130.86, 130.75, 130.67, 129.93, 129.14, 128.15, 122.92, 115.69, 115.48, 115.22, 115.01, 54.70, 51.03, 18.00.

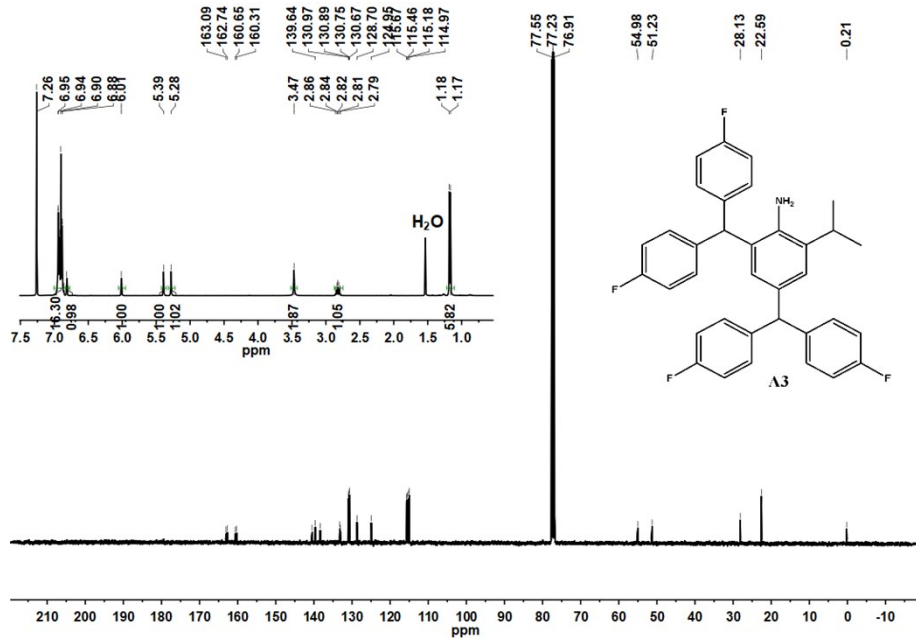
2-Ethyl-4,6-bis{di(*p*-fluorophenyl)methyl}aniline (A2, Yield: 73%)



Compound A2. ¹H NMR (400 MHz, CDCl₃, TMS): δ 6.99–6.88 (m, 16H), 6.77 (s, 1H, aryl-H), 6.07 (s, 1H, aryl-H), 5.41 (s, 1H, CH(*p*-FPh)₂), 5.30 (s, 1H, CH(*p*-FPh)₂), 3.46 (s, 2H, NH₂), 2.47 (q, *J* = 8 Hz, 2H, CH₂CH₃), 1.19 (t, *J* = 8 Hz, 3H, CH₂CH₃). ¹³C NMR (100 MHz,

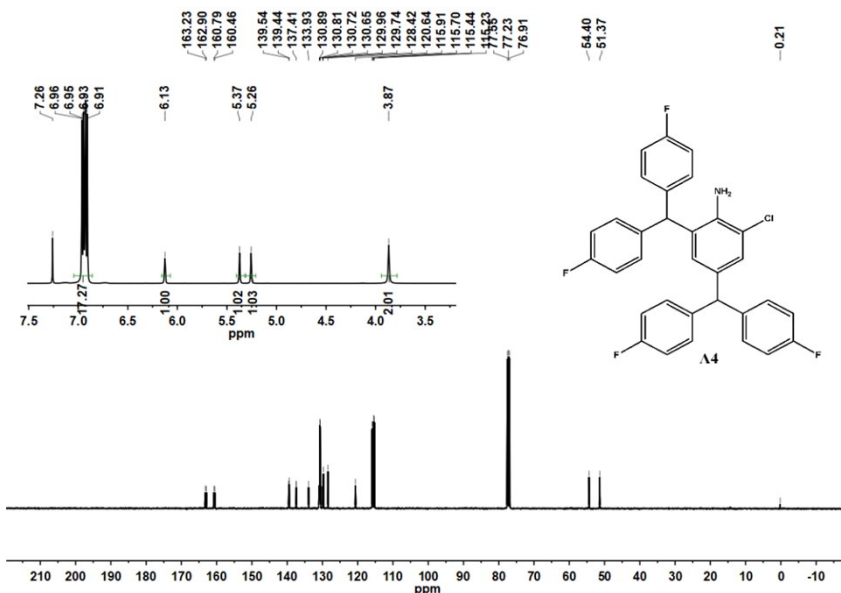
CDCl_3 , TMS): δ 163.08, 162.74, 160.64, 160.30, 140.38, 140.35, 140.32, 138.30, 138.27, 133.13, 130.94, 130.87, 130.75, 130.67, 128.98, 128.66, 128.42, 127.84, 115.68, 115.47, 115.20, 114.99, 54.87, 51.08, 24.53, 13.22.

2-Isopropyl-4,6-bis{di(*p*-fluorophenyl)methyl}aniline (A3**, Yield: 82%)**



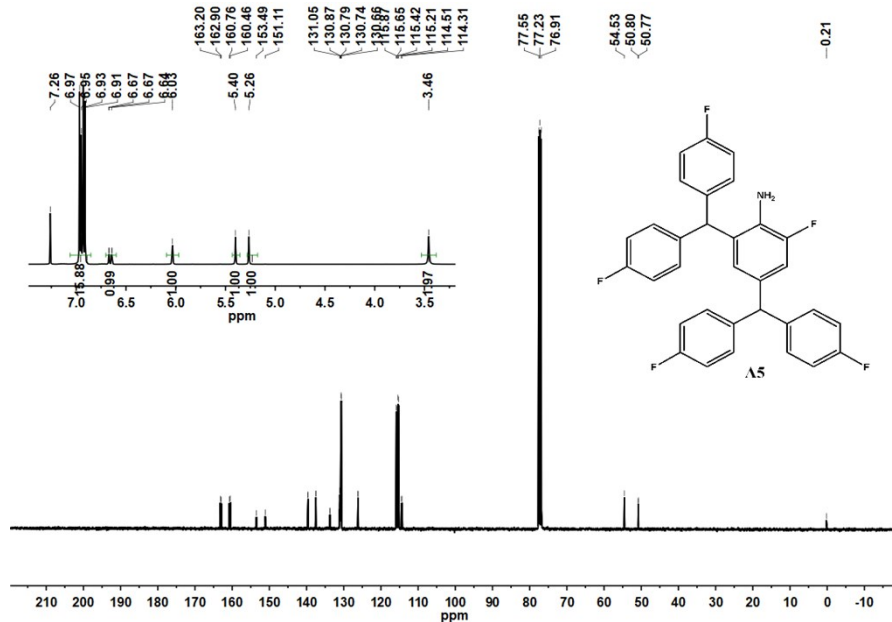
Compound A3. ^1H NMR (400 MHz, CDCl_3 , TMS): δ 6.95–6.86 (m, 16H), 6.82 (s, 1H, aryl-H), 6.01 (s, 1H, aryl-H), 5.39 (s, 1H, $\text{CH}(p\text{-FPh})_2$), 5.28 (s, 1H, $\text{CH}(p\text{-FPh})_2$), 3.47 (s, 2H, NH_2), 2.82 (m, 1H, $\text{CH}(\text{CH}_3)_2$), 1.17 (d, $J = 4$ Hz, 6H, $\text{CH}(\text{CH}_3)_2$). ^{13}C NMR (100 MHz, CDCl_3 , TMS): δ 163.09, 162.74, 160.65, 160.31, 140.46, 139.64, 138.34, 133.21, 133.07, 130.97, 130.89, 130.75, 130.67, 128.70, 128.64, 124.95, 115.67, 115.46, 115.18, 114.97, 54.98, 51.23, 28.13, 22.59.

2-Chloro-4,6-bis{di(*p*-fluorophenyl)methyl}aniline (A4**, Yield: 65%)**



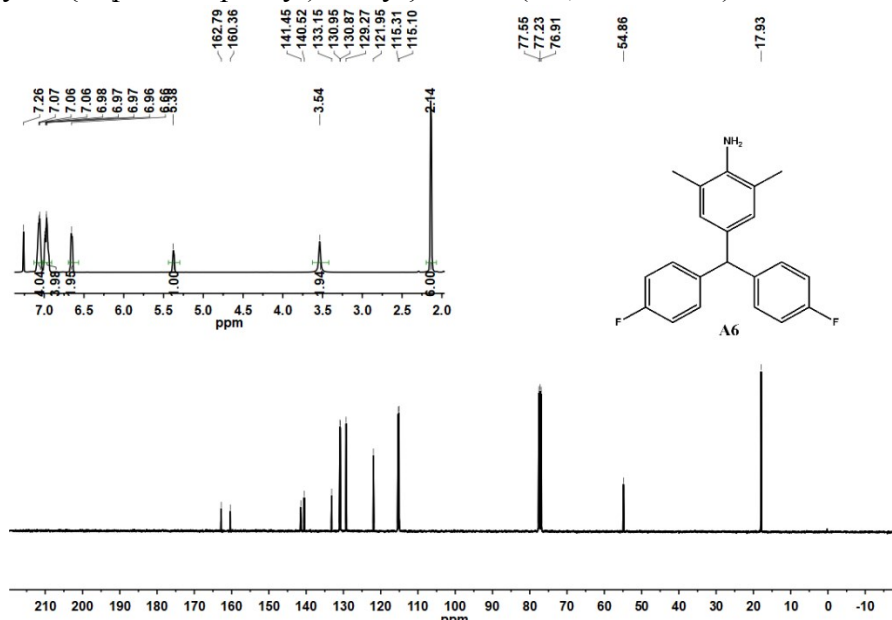
Compound A4. ^1H NMR (400 MHz, CDCl_3 , TMS): δ 6.96–6.91 (m, 17H), 6.13 (s, 1H), 5.37 (s, 1H, $\text{CH}(p\text{-FPh})_2$), 5.26 (s, 1H, $\text{CH}(p\text{-FPh})_2$), 3.87 (s, 2H, NH_2). ^{13}C NMR (100 MHz, CDCl_3 , TMS): δ 163.23, 162.90, 160.79, 160.46, 139.54, 139.44, 137.41, 133.93, 130.89, 130.81, 130.72, 130.65, 129.96, 129.74, 128.42, 120.64, 115.91, 115.70, 115.44, 115.23, 54.40, 51.37.

2-Fluoro-4,6-bis{di(*p*-fluorophenyl)methyl}aniline (A5**, Yield: 80%)**



Compound A5. ^1H NMR (400 MHz, CDCl_3 , TMS): δ 6.97–6.91 (m, 16H), 6.65 (d, $J = 6$ Hz, 1H), 6.03 (s, 1H, aryl-F), 5.40 (s, 1H, $\text{CH}(p\text{-FPh})_2$), 5.26 (s, 1H, $\text{CH}(p\text{-FPh})_2$), 3.46 (s, 2H, NH_2). ^{13}C NMR (100 MHz, CDCl_3 , TMS): δ 163.20, 162.90, 160.76, 160.46, 153.49, 151.11, 131.05, 130.87, 130.79, 130.74, 130.66, 130.65, 115.87, 115.65, 115.42, 115.21, 114.51, 114.31, 54.53, 50.80, 50.77.

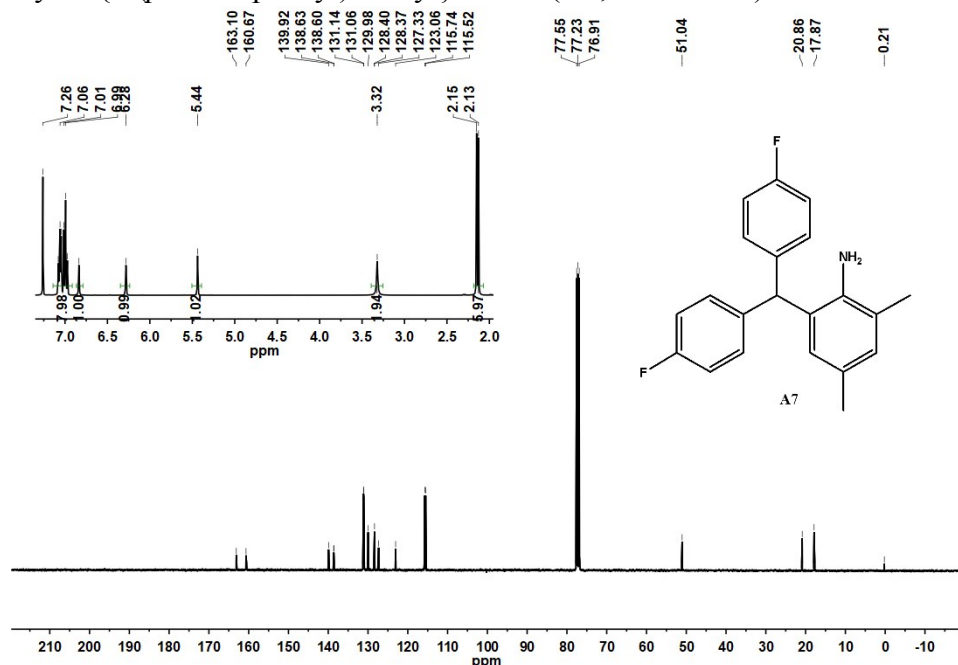
2,6-Dimethyl-4-{di(*p*-fluorophenyl)methyl}aniline (A6**, Yield: 69%)**



Compound A6. ^1H NMR (400 MHz, CDCl_3 , TMS): δ 7.07–6.95 (m, 8H), 6.66 (s, 2H, aryl-

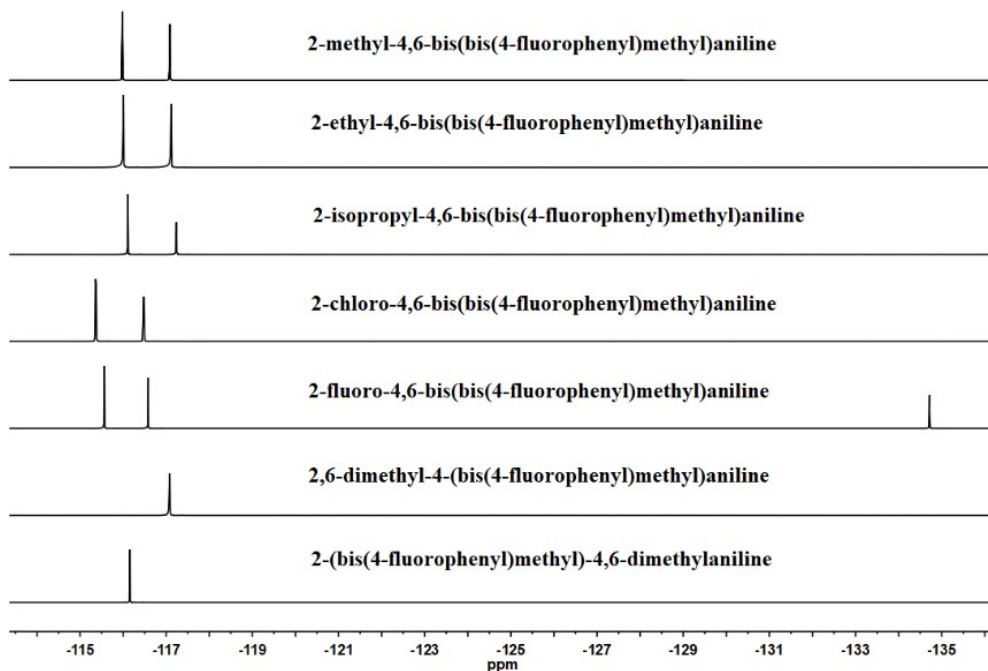
H), 5.38 (s, 1H, CH(*p*-FPh)₂), 3.54 (s, 2H, NH₂), 2.14 (s, 6H, 2 × CH₃). ¹³C NMR (100 MHz, CDCl₃, TMS): δ 162.79, 160.36, 141.45, 140.52, 133.15, 130.95, 130.87, 129.27, 121.95, 115.31, 115.10, 54.86, 17.93.

2,4-Dimethyl-6-{di(*p*-fluorophenyl)methyl}aniline (**A7**, Yield:65%)



Compound **A7**. ¹H NMR (400 MHz, CDCl₃, TMS): δ 7.08–6.97 (m, 8H), 6.84 (s, 1H, aryl-H), 6.28 (s, 1H, aryl-H), 5.44 (s, 1H, CH(*p*-FPh)₂), 3.32 (s, 2H, NH₂), 2.15 (s, 3H, CH₃), 2.13 (s, 3H, CH₃). ¹³C NMR (100 MHz, CDCl₃, TMS): δ 163.10, 160.67, 139.92, 138.63, 138.60, 131.14, 131.06, 129.98, 128.40, 128.37, 127.33, 123.06, 115.74, 115.52, 51.04, 20.86, 17.87.

(b) ¹⁹F NMR spectroscopic data for **A1 – A7**



A1: ¹⁹F NMR (470 MHz, CDCl₃): δ -115.98, -117.08.

A2: ^{19}F NMR (470 MHz, CDCl_3): δ –116.01, –117.12.

A3: ^{19}F NMR (470 MHz, CDCl_3): δ –116.11, –117.23.

A4: ^{19}F NMR (470 MHz, CDCl_3): δ –115.36, –115.37, –116.47, –116.48.

A5: ^{19}F NMR (470 MHz, CDCl_3): δ –115.56, –115.58, –134.72.

A6: ^{19}F NMR (470 MHz, CDCl_3): δ –117.08.

A7: ^{19}F NMR (470 MHz, CDCl_3): δ –116.16.

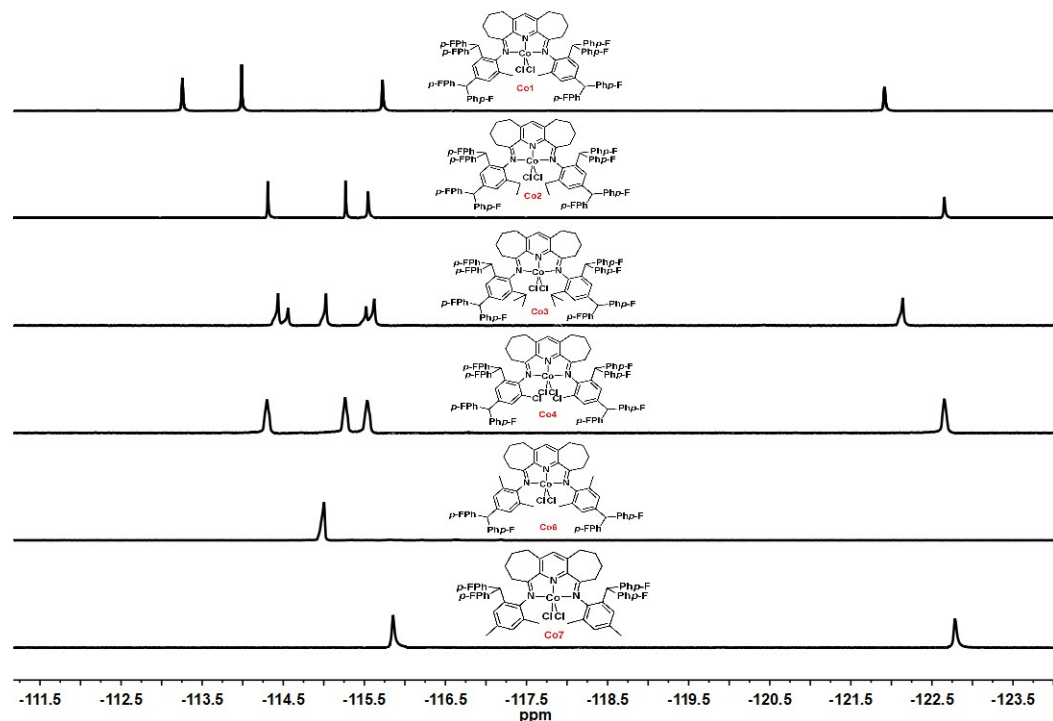


Figure S1. ^{19}F NMR spectra of **Co1**, **Co2**, **Co3**, **Co4**, **Co6** and **Co7**; recorded in CDCl_3 at ambient temperature.

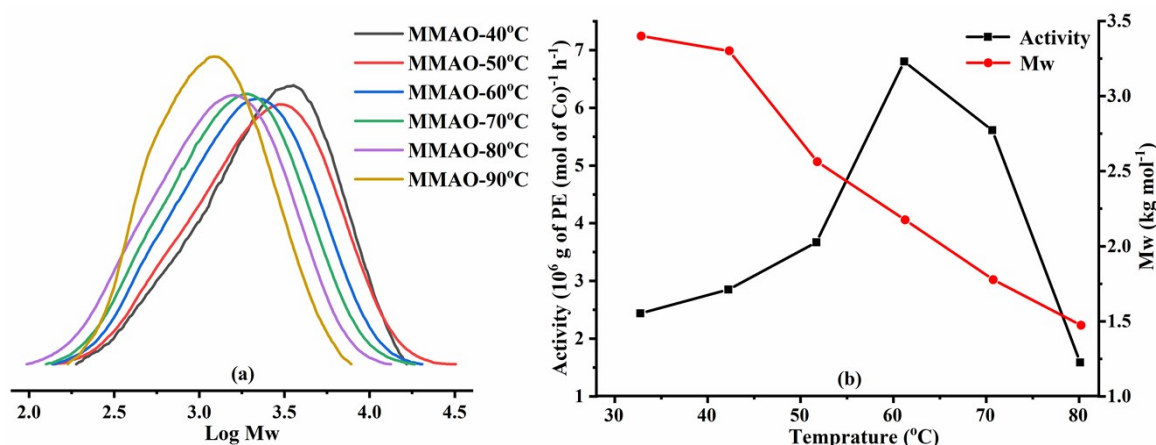


Figure S2. (a) GPC traces for the polymers obtained using **Co5**/MMAO at various temperatures; (b) Plot of activity and M_w versus temperature for the catalyst and polyethylene, respectively (entries 1 – 6, Table 4).

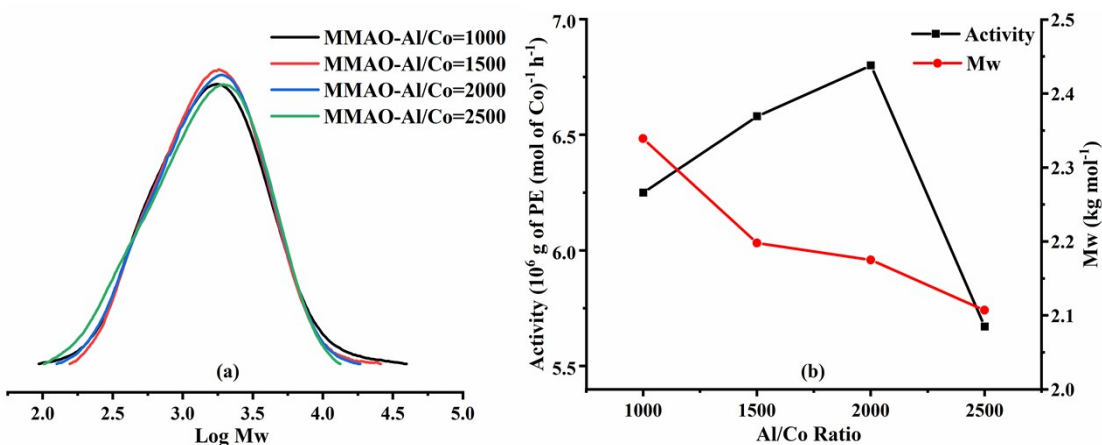


Figure S3. (a) GPC traces for the polymers obtained using **Co5**/MMAO at various Al:Co molar ratios; (b) Plot of activity and M_w versus Al:Co molar ratio for the catalyst and polyethylene, respectively (entries 4, 7 – 10, Table 4).

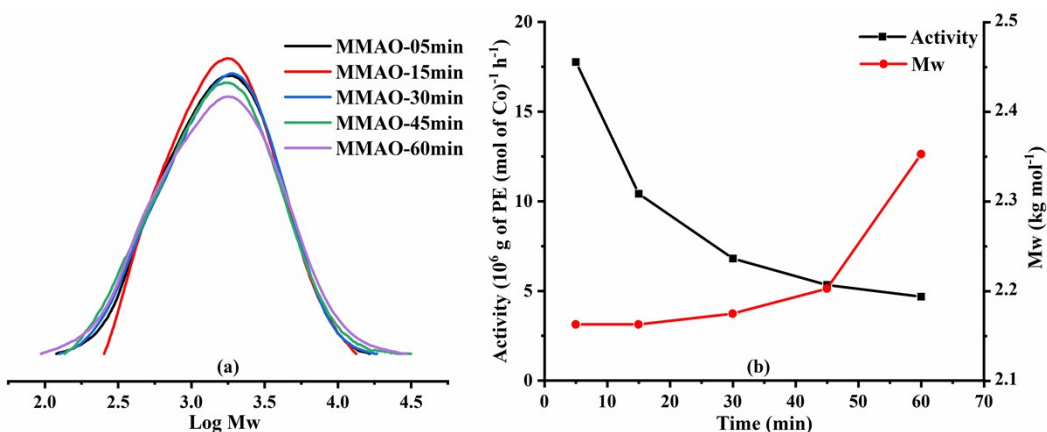


Figure S4. (a) GPC traces for the polymers obtained using **Co5**/MMAO at various times; (b) Plot of activity and M_w versus time for the catalyst and polyethylene, respectively (entries 4, 11 – 14, Table 4).

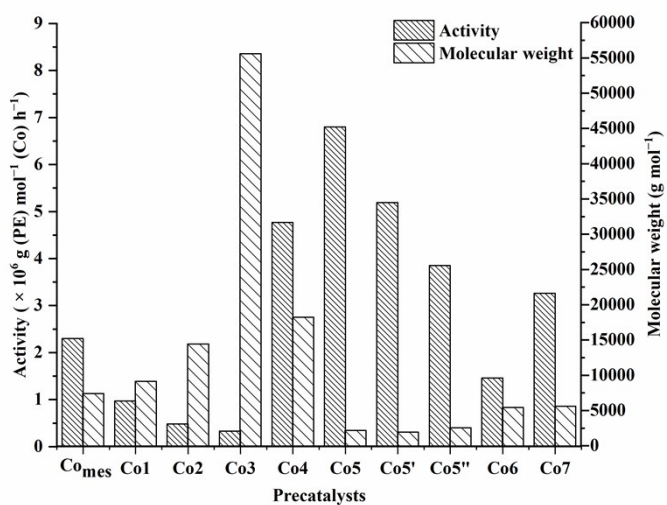


Figure S5. Comparison of the catalytic activities and molecular weight of the polyethylenes generated using **Co1** – **Co7** and **Co_{mes}**; MMAO used as co-catalyst in each case.

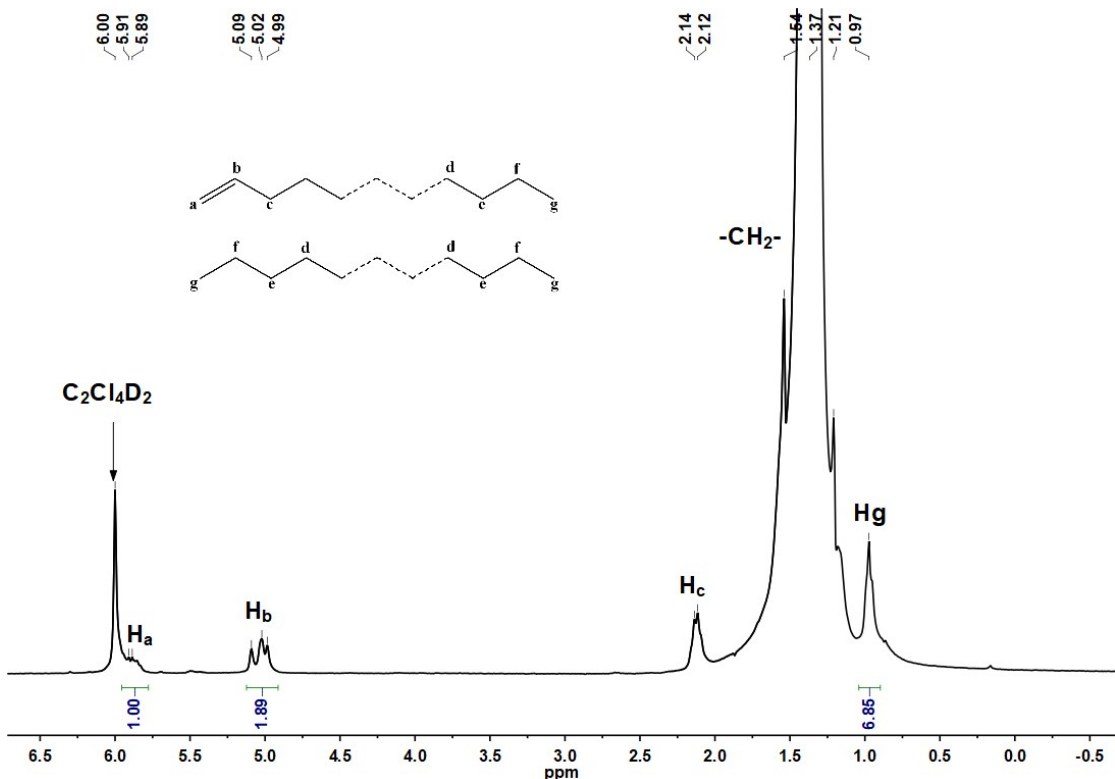


Figure S6. ¹H NMR spectrum of the polyethylene obtained using **Co4**/MAO at 60 °C; recorded at 100 °C in 1,1,2,2-tetrachloroethane-*d*₂ (entry 5, Table 3).

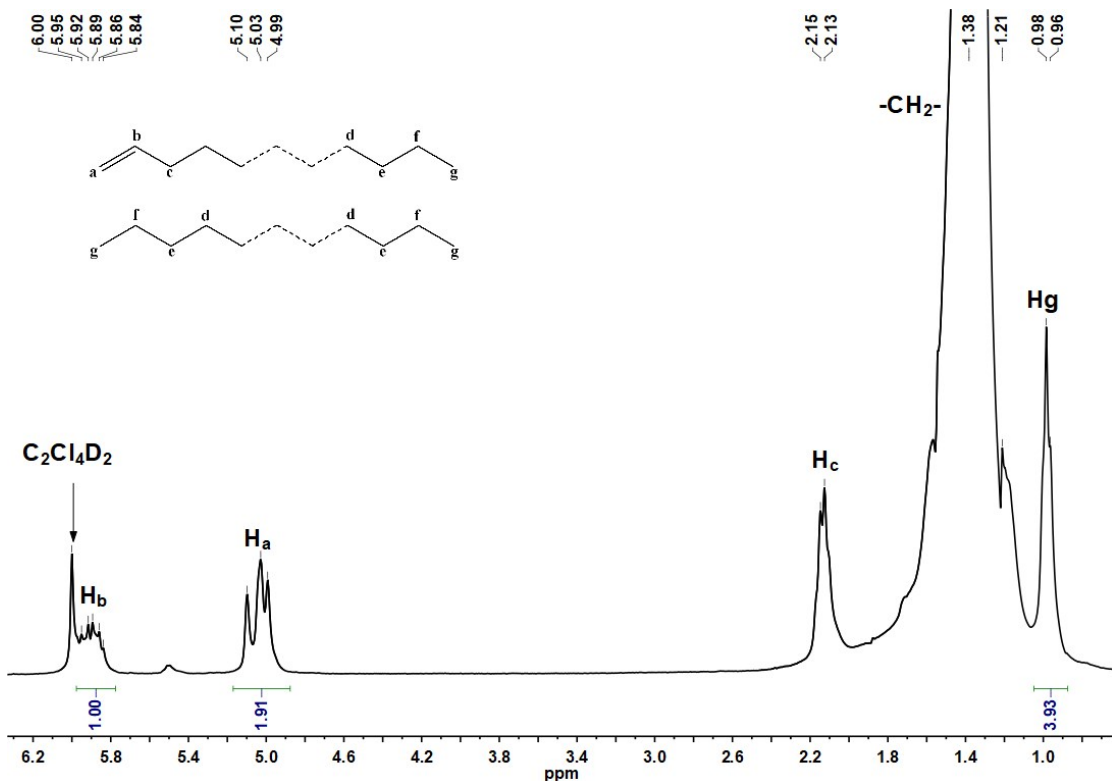


Figure S7. ¹H NMR spectrum of the polyethylene obtained using **Co5'**/MAO at 60 °C; recorded at 100 °C in 1,1,2,2-tetrachloroethane-*d*₂ (entry 7, Table 3).

Table S1. Crystal data and structure refinements for **Co4**, **Co5**, **Co5'** and **Co5''**

	Co4	Co5	Co5'	Co5''
CCDC Number	1998230	1998231	1998232	1998233
Empirical formula	$2(\text{C}_{79}\text{H}_{57}\text{C}_{14}\text{CoF}_8\text{N}_3)$	$2(\text{C}_{79}\text{H}_{57}\text{Cl}_2\text{CoF}_{10}\text{N}_3 \cdot \text{C}_4\text{H}_{10}\text{O})$	$\text{C}_{81}\text{H}_{60}\text{ClCoF}_{10}\text{N}_3\text{O}_2$	$\text{C}_{79}\text{H}_{65}\text{Cl}_2\text{CoF}_2\text{N}_3 \cdot \text{C}_4\text{H}_8\text{O} \cdot \text{CH}_2\text{Cl}_2$
Formula weight	2802.01	2810.32	1391.70	1381.20
Temperature/K	169.99(10)	169.99(12)	169.99(11)	169.99(12)
Crystal system	monoclinic	monoclinic	monoclinic	triclinic
Space group	P2 ₁ /c	P2 ₁ /c	P2 ₁ /c	P-1
a/Å	16.65280(10)	15.6079(2)	18.5816(3)	10.4294(4)
b/Å	25.4947(2)	28.3387(4)	27.4361(2)	18.2182(7)
c/Å	35.8638(2)	33.8316(5)	16.5226(3)	20.3353(7)
$\alpha/^\circ$	90	90	90	65.813(4)
$\beta/^\circ$	97.8590(10)	92.5730(10)	116.265(2)	76.760(4)
$\gamma/^\circ$	90	90	90	81.879(3)
Volume/Å ³	15083.25(17)	14948.9(4)	7553.7(2)	3426.0(2)
Z	4	4	4	2
$\rho_{\text{calc}}/\text{g/cm}^3$	1.234	1.249	1.224	1.339
μ/mm^{-1}	3.607	3.043	2.704	3.840
F(000)	5752.0	5792.0	2868.0	1442.0
Crystal size/mm ³	0.225 × 0.145 × 0.078	0.38 × 0.27 × 0.15	0.519 × 0.256 × 0.089	0.25 × 0.15 × 0.05
2θ range for data collection/°	CuKα ($\lambda = 1.54184$)	CuKα ($\lambda = 1.54184$)	CuKα ($\lambda = 1.54184$)	CuKα ($\lambda = 1.54184$)
Index ranges	4.974 to 151.166	5.23 to 151.272	5.304 to 151.278	4.852 to 151.946
Reflections collected	-20 ≤ h ≤ 20, -31 ≤ k ≤ 27, -44 ≤ l ≤ 44	-19 ≤ h ≤ 19, -35 ≤ k ≤ 34, -36 ≤ l ≤ 42	-19 ≤ h ≤ 21, -34 ≤ k ≤ 34, -20 ≤ l ≤ 20	-12 ≤ h ≤ 13, -22 ≤ k ≤ 22, -25 ≤ l ≤ 24
Independent reflections	108973	109151	48495	47515
Data/restraints/parameters	30074 [$R_{\text{int}} = 0.0477$, $R_{\text{sigma}} = 0.0424$]	29571 [$R_{\text{int}} = 0.0524$, $R_{\text{sigma}} = 0.0422$]	14476 [$R_{\text{int}} = 0.0501$, $R_{\text{sigma}} = 0.0349$]	13523 [$R_{\text{int}} = 0.0813$, $R_{\text{sigma}} = 0.0759$]
Goodness-of-fit on F^2	30074/169/1748	29571/0/1758	14476/867/1173	13523/0/858
Final R indexes [I>=2σ (I)]	1.016	1.031	1.049	1.238
Final R indexes [all data]	$R_1 = 0.0569$, $wR_2 = 0.1476$	$R_1 = 0.0919$, $wR_2 = 0.2534$	$R_1 = 0.1101$, $wR_2 = 0.2728$	$R_1 = 0.1134$, $wR_2 = 0.3074$
Largest diff. peak/hole / e Å ⁻³	$R_1 = 0.0747$, $wR_2 = 0.1607$	$R_1 = 0.1127$, $wR_2 = 0.2680$	$R_1 = 0.1508$, $wR_2 = 0.3026$	$R_1 = 0.1370$, $wR_2 = 0.3290$
Flack parameter	0.41/-0.34	1.22/-0.72	0.55/-0.39	2.16/-1.50

References

- 1 (a) S. Meiries, K. Speck, B. D. Cordes, A. M. Z. Slawin and S. P. Nolan, *Organometallics*, 2013, **32**, 330–339; (b) P. Shaw, A. R. Kennedy and D. J. Nelson, *Dalton Trans.*, 2016, **45**, 11772–11780.